Water-Dispersible Polymer/Pd/Ni Hybrid Magnetic Nanofibers

Xiaohu Yan and Guojun Liu*

Department of Chemistry, Queen's University, 60 Bader Lane, Kingston, Ontario, Canada K7L 3N6

Matthias Haeussler and Ben Zhong Tang

Department of Chemistry, Hong Kong University of Science & Technology, Clear Water Bay, Kowloon, Hong Kong, China

Received July 15, 2005. Revised Manuscript Received September 21, 2005

Reported are the preparation and characterization of Pd/Ni nanoparticles in the core of water-dispersible nanotubes of a triblock copolymer. The preparation involves first the preparation of the triblock nanotubes and then the production of Pd nanoparticles inside the nanotube cores. Ni is introduced in the final step by electroless deposition using Pd as the catalyst. The challenges facing each reaction step are discussed.

I. Introduction

Solvent-dispersible block copolymer/inorganic magnetic nanofibers can be prepared by loading into the tubular core of block copolymer nanotubes with γ-Fe_2O_3, Ni, or Co, etc. We previously reported the preparation of superparamagnetic polymer/γ-Fe_2O_3 nanofibers by loading γ-Fe_2O_3 into the cores of polystyrene-*block*-poly(2-cinnamoyloxyethyl methacrylate)-*block*-poly(acrylic acid) or PS−PCEMA−PAA nanotubes, where PS made up the corona or the outermost layer of the tubes, the cross-linked PCEMA constituted the tubular wall, and PAA stretched from the inner surface of the tubular wall into the center of the tubes.[1] Polymer/inorganic magnetic nanofibers have interesting properties. The PS−PCEMA−PAA/γ-Fe_2O_3 fibers, for example, dispersed in a wide range of organic solvents including tetrahydrofuran (THF) and responded to an applied magnetic field, on one hand, by aligning themselves in the field and, on the other hand, by attracting one another to form fiber bundles.[2] These fibers can, in principle, be connected covalently in a controlled fashion to other nano- or microstructures to yield complex "superstructures", a task that was recently accomplished by us for block copolymer nanotubes.[2] Using an appropriate superstructure design and making use of the magnetic response of the magnetic hybrid nanofibers, we should, in principle, be able to prepare nanomechanical devices that are driven by an on−off external magnetic field. For the preparation of potential nanomechanical devices that operate in an aqueous environment, water-dispersible polymer/inorganic magnetic nanofibers are required. This paper reports the preparation of water-dispersible polymer/Pd/Ni hybrid magnetic nanofibers.

The fibers were derived from nanotubes prepared from poly(glyceryl methacrylate)-*block*-poly[(2-cinnamoyloxyethyl methacrylate)-*ran*-(2-hydroxyethyl methacrylate)]-*block*-poly(*tert*-butyl acrylate) or PGMA−P(CEMA−HEMA)−P*t*BA, where $n = 3.8 \times 10^2$, $m = 123$, $l = 119$, and $x = 65\%$. This triblock was chosen for nanotube preparation for the water solubility of the PGMA block, the photo-cross-linkability of the CEMA units, and the ready hydrolysis of tBA. We did not fully cinnamate the precursory PHEMA block and prepared a P(CEMA−HEMA) block rather than a PCEMA block mainly to retain the compatibility of this block with metal ions such as Pd(II) and Ni^{2+}. To prepare the nanotubes, we first dispersed the triblock in water to yield cylindrical aggregates, where the PGMA block formed the corona, the P(CEMA−HEMA) block constituted the insoluble intermediate layer, and the P*t*BA block formed the tubular core (A → B, Scheme 1). The aggregates in water were then photolyzed to cross-link the P(CEMA−HEMA) intermediate layer and lock in the cylindrical structure (B → C). Nanotubes with poly(acrylic acid)- or PAA-lined cores were obtained after the hydrolysis of the P*t*BA core (C → D). We introduced Pd(II) into the core by stirring such nanotubes with $PdCl_2$, which led to Pd(II) complexation with the AA groups of the PAA chains. Pd(0) nanoparticles were produced by Pd(II) reduction via the addition of $NaBH_4$ (D → E). Pd then served as the catalyst for Ni deposition by electroless plating (E → F) to yield polymer/Pd/Ni hybrid nanofibers.

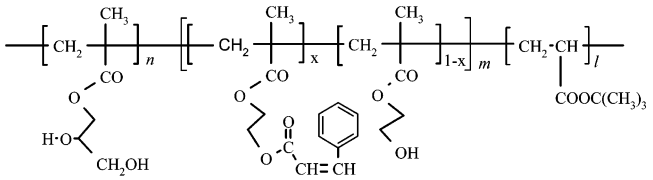

PGMA-P(CEMA-HEMA)-P*t*BA

Although the polymer/metal hybrid magnetic structures described here are new, there have been many reports on surfactant-stabilized[3] and bare[4] metal nanowires. There have also been some reports on the preparation of block copolymer

* Corresponding author e-mail: gliu@chem.queensu.ca.

(1) Yan, X. H.; Liu, G. J.; Liu, F. T.; Tang, B. Z.; Peng, H.; Pakhomov, A. B.; Wong, C. Y. *Angew. Chem., Int. Ed.* **2001**, *40*, 3593.

(2) (a) Liu, G. J.; Yan, X. H.; Li, Z.; Zhou, J. Y.; Duncan S. *J. Am. Chem. Soc.* **2003**, *125*, 14039. (b) Yan, X. H.; Liu, G. J.; Li, Z. *J. Am. Chem. Soc.* **2004**, *126*, 10059.

10.1021/cm051548d CCC: $30.25
Published on Web 11/05/2005

Scheme 1. Schematic Illustration of the Formation and Chemical Processing of a PGMA−P(CEMA−HEMA)−P*t*BA Cylindrical Aggregate with One Exposed End[a]

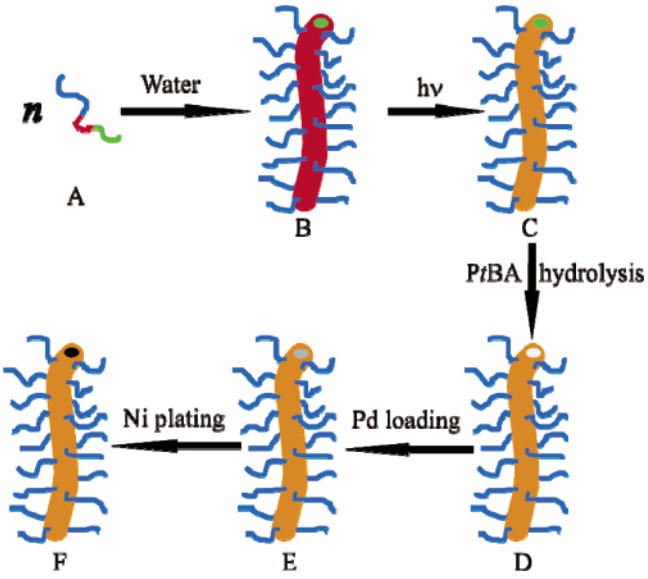

[a] In reality, the two ends of a cylindrical aggregate are capped by PGMA−P(CEMA-HEMA)−P*t*BA hemispheres.

nanotubes[5−10] and nanofibers.[11,12] More recently, there have appeared reports on the loading of CdS,[13] Ag,[14] and Pd[15] into the core of block copolymer nanotubes. Aside from the preparation of solvent-dispersible polymer/inorganic hybrid nanofibers, metal oxides such as γ-Fe_2O_3,[16] semiconductors such as CdS,[16] and metals such as Co[17] and Ni[18] have also been introduced into the tubular channels of diblock thin films to yield polymer/inorganic composite films. To introduce metals in the latter cases, electrodeposition was typically used.

II. Experimental Section

Materials and Reagents. Except hydrochloric acid (36.5−38%, Fisher Sci.), anhydrous ethanol (Fisher Sci.), *N*,*N*-dimethylformamide (99.9%, DM, Fisher Sci,), diethyl ether (99.9%, Fisher Sci.), and ammonia (28−30%, Caledon Laboratories), all other reagents were purchased from Aldrich. $PdCl_2$ (99%), $NaBH_4$ (98%), $(C_2H_5)_3SiH$ (99%, triethylsilane), $CH_3C(=NOH)C(=NOH)CH_3$ (99+%, dimethylglyoxime), $HOC(COOH)(CH_2COOH)_2$ (99%, citric acid), KCl (99+%), $NiSO_4 \cdot 6H_2O$ (99%), $NiCl_2 \cdot 6H_2O$, NH_4Cl (99+%), $Na_2H_2PO_2 \cdot 2H_2O$, $C_{10}H_{14}N_2O_8Na_2$ (99.0−101.0%, ethylenediaminetetraacetic acid disodium salt dihydrate or EDTA disodium salt), NH_2NH_2 (98%, hydrazine), CF_3COOH (99%), and $Na_2HC_6H_5O_7 \cdot 1.5H_2O$ (99%, sodium hydrogen citrate sesquihydrate) were all used as received.

PGMA−P(CEMA−HEMA)−P*t*BA was prepared following procedures reported before.[2b] It was derived from PSMA−PHEMA−P*t*BA, where PSMA denotes poly(solketyl methacrylate). The first step involved the partial cinnamation of the PHEMA block by cinnamoyl chloride. PSMA was then hydrolyzed in THF containing hydrochloric acid. After hydrolysis, the sample was dialyzed against methanol for solvent switch.

PSMA−PCEMA−P*t*BA Characterization. The triblock copolymer PGMA−P(CEMA−HEMA)−P*t*BA was characterized in the PSMA−PCEMA−P*t*BA form for the better solubility of the PSMA and PCEMA blocks in solvents such as THF and $CDCl_3$. SEC was performed using THF as the eluant. The Waters HT-4 column used was calibrated using monodisperse poly(methyl methacrylate) standards. The refractive index difference Δn_r between polymer solution and solvent THF was measured using light that had passed through a 633-nm band-pass filter on a Phoneix Precision instrument. The specific refractive index increment dn_r/dc was determined from the intercept of a straight line obtained from plotting $\Delta n_r/c$ vs c, where c denotes the copolymer concentration in THF. The weight-average molar mass was measured in THF using a light scattering instrument (Brookhaven model 9025) equipped with a 632.8 nm He−Ne laser. ^{1}H NMR spectra of PSMA−P(CEMA−HEMA)−P*t*BA and PSMA−PCEMA−P*t*BA were measured in $CDCl_3$ using a Bruker AC200 instrument.

Block Copolymer Nanotube Preparation. PGMA−P(CEMA−HEMA)−P*t*BA, 150 mg, dissolved in methanol was added into diethyl ether to precipitate the polymer. After the supernatant was decanted, 80 mL of distilled water was added. The mixture was stirred magnetically for 4 days before being heated at 80 °C for 24 h under a N_2 atmosphere. The final mixture was centrifuged at 1550*g* for 10 min to remove the part that did not disperse. The supernatant was irradiated under stirring at 20 °C with a focused UV beam from a 500 W mercury lamp to effect a CEMA double-bond conversion of ~30%. The CEMA double-bond conversion was determined from an absorbance decrease of CEMA at 274 nm.

Hydrolysis of PtBA needed to be performed in an aprotic solvent such as CH_2Cl_2. For solvent switch, we first dialyzed a solution of the cross-linked cylindrical aggregates or nanofibers against methanol to remove water. The resulting methanol solution was added into anhydrous diethyl ether to precipitate out the nanofibers. The fibers were rinsed with three aliquots of diethyl ether before dichloromethane and trifluoroacetic acid (v/v = 75/25) containing triethylsilane at 2.5 molar equivalents relative to the *t*BA groups was added. This mixture was stirred for 2 h before it was centrifuged

(3) See, for example, Xia, Y. N.; Yang, P. D.; Sun, Y. G.; Wu, Y. Y.; Mayers, B.; Gates, B.; Yin Y. D.; Kim, F.; Yan, Y. Q. *Adv. Mater.* **2003**, *15*, 353.
(4) See, for example, (a) Lieber, C. M. *MRS Bull.* **2003**, *28*, 486. (b) Kovtyukhova, N. I.; Mallouk, T. E. *Chem. Eur. J.* **2002**, *8*, 4355.
(5) Stewart, S.; Liu, G. J. *Angew. Chem., Int. Ed.* **2000**, *39*, 340.
(6) Yan, X. H.; Liu, F. T.; Li, Z.; Liu, G. J. *Macromolecules* **2001**, *34*, 9112.
(7) Yu, K.; Zhang, L. F.; Eisenberg, A. *Langmuir* **1996**, *12*, 5980.
(8) (a) Raez, J.; Barjovanu, R.; Massey, J. A.; Winnik, M. A.; Manners, M. A. *Angew. Chem., Int. Ed.* **2000**, *39*, 3862. (b) Raez, J.; Manners, I.; Winnik, M. A. *J. Am. Chem. Soc.* **2002**, *124*, 10381.
(9) Jenekhe, S.; Chen, L. *Science* **1998**, *279*, 1903.
(10) Grumelard, J.; Taubert, A.; Meier, W. *Chem. Commun.* **2004**, *1462*.
(11) Dalhaimer, P.; Bates, F. S.; Discher, D. E. *Macromolecules* **2003**, *36*, 6873.
(12) See, for example, (a) Liu, G. J.; Qiao, L. J.; Guo, A. *Macromolecules* **1996**, *29*, 5508. (b) Liu, G. J.; Ding, J. F.; Qiao, L. J.; Guo, A.; Gleeson, J. T.; Dymov, B.; Hashimoto, T.; Saijo, K. *Chem. Eur. J.* **1999**, *5*, 2740. (c) Massey, J.; Power, K. N.; Manners, I.; Winnik, M. A. *J. Am. Chem. Soc.* **1998**, *120*, 9533. (d) Won, Y.-Y.; Davis, H. T.; Bates, F. S. *Science* **1999**, *283*, 960. (e) Templin, M.; Franck, A.; DuChesne, A.; Leist, H.; Zhang, Y. M.; Ulrich, R.; Schadler, V.; Wiesner, U. *Science* **1997**, *278*, 5344. (f) Lei, L. C.; Gohy, J. F.; Willet, N.; Zhang, J. X.; Varshney, S.; Jerome, R. *Macromolecules* **2004**, *37*, 1089. (g) de Moel, K.; van Ekenstein, G.; Nijland, H.; Polushkin, E.; ten Brinke, G.; Maki-Ontto, R.; Ikkala, O. *Chem. Mater.* **2001**, *13*, 4580.
(13) Duxin, N.; Liu, F. T.; Vali, H.; Eisenberg, A. *J. Am. Chem. Soc.* **2005**, *127*, 10063.
(14) Wang, X. S.; Wang, H.; Coombs, N.; Winnik, M. A.; Manners, M. A. *J. Am. Chem. Soc.* **2005**, *127*, 8924.
(15) Li, Z.; Liu, G. J. *Langmuir* **2003**, *19*, 10480.
(16) Liu, G. J.; Ding, J. F.; Hashimoto, T.; Saijo, K.; Winnik, F. M.; Nigam, S. *Chem. Mater.* **1999**, *11*, 2233.
(17) Thurn-Albrecht, T.; Schotter, J.; Kastle, C. A.; Emley, N.; Shibauchi, T.; Krusin-Elbaum, L.; Guarini, K.; Black, C. T.; Tuominen, M. T.; Russell, T. P. *Science* **2000**, *290*, 2126.
(18) Sidorenko, A.; Tokarev, I.; Minko, S.; Stamm, M. *J. Am. Chem. Soc.* **2003**, *125*, 12211

Table 1. Recipes for the Plating Solution Components

Ni^{2+} solution		reductant solution	
reagent	amount	reagent	amount
$NiCl_2 \cdot 6H_2O$	0.590 g	$Na_2H_2PO_2 \cdot 2H_2O$	0.739 g
$NiSO_4 \cdot 6H_2O$	0.240 g	H_2O	10.0 mL
$Na_2HC_6H_5O_7 \cdot 1.5H_2O$	0.142 g		
NH_4Cl	1.00 g		
H_2O	10.0 mL		

at 1550*g* to settle the sample. The sample was re-dispersed in methanol and precipitated in diethyl ether to remove the residual acid. This process was repeated twice. The nanotubes were eventually dispersed in DMF for storage.

Palladium Loading. A DMF solution of the nanotubes at ~10 mg/mL was de-oxygenated for 10 min by nitrogen bubbling. Solid $PdCl_2$ was then added under nitrogen bubbling at 0.4 to ~2 mg/mL. This mixture was stirred overnight before it was dialyzed under nitrogen protection against water changed 5 times over 24 h. An aqueous $NaHB_4$ solution at approximately 2 times excess was dropped in over 1−2 min. This caused an immediate color change from gray to black. After 2 h, the solution was dialyzed against distilled water and changed 3 times over 10 h to remove excess reductant.

To monitor the kinetics of palladium loading into the nanotube cores, 1.00 mL of a nanotube solution in DMF (13.2 mg, 0.0168 mmol carboxyl group) was mixed with 20.00 mL of a $PdCl_2$ (2.26 mg, 0.0127 mmol) solution in DMF. At pre-designated times, 2 mL of the mixture was taken out and filtered through a 0.2 μm pore size PTFE filter (Whatman Co.). Of the filtrate 1.00 mL was used to prepare a complex with dimethylglyoxime under controlled acidic conditions following a literature method.[27] The water-insoluble complex was then extracted by chloroform for absorbance analysis at 380 nm to quantify Pd^{2+} that had not been complexed with the nanotubes.

Ni Plating. The nickel plating solution recipe was taken from the literature.[19]

It consisted of two parts (Table 1): the Ni^{2+} solution and the reductant solution. The pH of the Ni^{2+} solution was at 8.75.

A typical procedure involved first adjusting the pH to 8.75 of a nanotube solution at ~3 mg/mL by adding 0.1 M ammonia solution. This was followed by the addition in aliquots of a calculated amount of the Ni^{2+} and reductant solutions at v/v = 1.00/1.00. To add a total of 0.67 mL of the Ni^{2+} solution in one experiment, for example, we divided this amount into four aliquots. The first aliquot consisted of 0.20 mL of the Ni^{2+} solution. The plating mixture was stirred for 2 h before the second aliquot at 0.20 mL was added. The addition of this was followed by the third and fourth aliquots at 0.20 and 0.16 mL, respectively, with a half-an-hour interval between additions. The final mixture was stirred overnight before it was dialyzed against water changed 4 to 5 times over 24 h under nitrogen protection to clean the sample. For thermogravimetric analysis (TGA) and magnetic property measurement, the plated samples were precipitated into THF and dried under vacuum.

Table 2. Characteristics of PSMA−PCEMA−P*t*BA

dn_r/dc (mL/g)	LS M_w (g/mol)	SEC M_w/M_n	NMR *n*/*m*/*l*	n	m	l
0.100	12.2×10^4	1.03	1.00/0.33/0.32	3.8×10^2	123	119

Thermogravimetric Analyses. The TGA analyses were carried out with a NETZSCH STA 449C instrument. The temperature was ramped up from 20 to 600 °C in a nitrogen atmosphere at 10 °C/min and then held at 600 °C for 10 min. The metal content in a polymer/metal sample was calculated using an equation derived before[20] based on the assumption that the residual weight fraction in such a sample was derived from carbonized polymer and the inert metal.

TEM and Magnetic Property Measurements. Transmission electron microscopy (TEM) images were obtained using a Hitachi H-7000 instrument operated at 75 kV. All of the samples were aspirated as aqueous dispersions on carbon-coated copper grids using a homemade device.[21] The polymer/Pd/Ni nanofibers with 51.5 and 68.4 wt % of Ni did not disperse well in water and were ultrasonicated for 5 min before aspiration. All samples were stained by OsO_4 vapor for 2−4 h before observation. Magnetic properties of the polymer/Pd/Ni solid samples were measured by a vibrating sample magnetometer (ADE Technologies).

III. Results and Discussion

Characteristics of the Polymer. LS, SEC, and NMR were used to characterize the triblock copolymer used. To ensure dissolution of the polymer in solvents such as THF and $CDCl_3$, the polymer was characterized in the PSMA−PCEMA−P*t*BA form whenever possible. Table 2 summarizes the characteristics of the PSMA−PCEMA−P*t*BA polymer.

The specific refractive index increment dn_r/dc and SEC polydispersity index M_w/M_n of the PSMA−PCEMA−P*t*BA sample were determined in THF and are 0.100 mL/g and 1.03, respectively. Since M_w/M_n was determined based on poly(methyl methacrylate) standards and could be erroneous, we calculated only the weight-average number of repeat units for each block by combining the LS M_w and NMR number of repeat unit ratio *n*/*m*/*l*. These values are 3.8×10^2, 123, and 119, respectively, for the PSMA, PCEMA, and P*t*BA blocks. By comparing the NMR spectra of PSMA−P(CEMA−HEMA)−P*t*BA and PSMA−PCEMA−P*t*BA, we determined a PHEMA degree of cinnamation efficiency of 65% for PSMA−P(CEMA−HEMA)−P*t*BA.

PGMA−P(CEMA−HEMA)−P*t*BA Cylindrical Aggregates. To produce cylindrical aggregates from PGMA−P(CEMA−HEMA)−P*t*BA with structure depicted in Scheme 1, we stirred a freshly precipitated PGMA−P(CEMA−HEMA)−P*t*BA sample with water first at room temperature for 4 days and then at 80 °C for 1 day. Figure 1 shows a TEM image of the resultant aggregates after being aspirated from water onto a carbon-coated copper grid. Not only the simple cylindrical aggregates but also branched cylinders, loops, and spherical aggregates coexisted in the sample. It should, however, be realized that Figure 1 was chosen mainly to show the diversity in the shapes of the aggregates and not the relative population of the different species. The

(19) Caturla, F.; Molina, F.; Molina-Saio, M. *J. Electrochem. Soc.* **1995**, *142*, 4084.
(20) Underhill, R. S.; Liu, G. J. *Chem. Mater.* **2000**, *12*, 2082.
(21) Ding, J. F.; Liu, G. J. *Macromolecules* **1999**, *32*, 8413.
(22) Brandrup, J.; Immergut, E. H. *Polymer Handbook*, 3rd ed.; John Wiley & Sons: New York, 1989.
(23) (a) Henselwood, F.; Wang, G. C.; Liu, G. J. *J. Appl. Polym. Sci.* **1998**, *70*, 397. (b) Wang, G. C.; Henselwood, F.; Liu, G. J. *Langmuir* **1998**, *14*, 1554.
(24) Lu, Z. H.; Liu, G. J.; Duncan, S. *Macromolecules* **2004**, *37*, 174.
(25) Lu, Z. H.; Liu, G. J.; Phillips, H.; Hill, J. M.; Chang, J.; Kydd, R. A. *Nano Lett.* **2001**, *1*, 683.
(26) See, for example, (a) Segregina, M. V.; Bronstein, L. M.; Platonova, O. A.; Chernyshov, D. M.; Valetsky, P. M. *Chem. Mater.* **1997**, *9*, 923. (b) Mossmer, S.; Spatz, J. P.; Moller, M.; Aberle, T.; Schmidt, J.; Burchard, W. *Macromolecules* **2000**, *33*, 4791.
(27) Yan, X. H.; Liu, G. J.; Li, H. X. *Langmuir* **2004**, *20*, 4677.

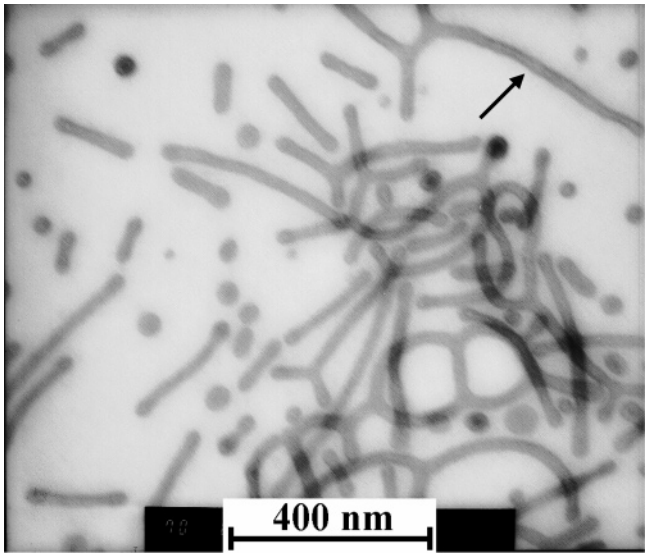

Figure 1. TEM image of PGMA−P(CEMA−HEMA)−P*t*BA cylindrical aggregates. The sample was stained by OsO_4.

analysis of many other TEM images by us revealed that the simple straight cylinders were by far the most dominant under the preparation conditions. For the dominance of the cylindrical aggregates, we will refer to the aggregates from now on collectively as "cylindrical aggregates". This is, by no means, to suggest the morphological uniformity of the aggregates.

Since the sample was stained by the CEMA-specific agent OsO_4, we anticipated the observation of core−shell dark-light cylinders with P(CEMA−HEMA) making up the shell and P*t*BA the core. This core−shell contrast was seen for some cylinders as marked for one cylinder in Figure 1 but was, unfortunately, not always clear. Suspecting that P(CEMA−HEMA) and P*t*BA were not fully segregated for the glass transition temperatures of 69 °C for PCEMA[12b] and 73 °C for P*t*BA,[22] we heated the sample at 80 °C for 24 h. Unfortunately, this treatment did not lead to a noticeable improvement in the core−shell contrast. Thus, our speculation is that the core−shell contrast was not sharp for the low concentration of double bonds in the P(CEMA−HEMA) layer.

The heat treatment did not change the size of the P*t*BA/P(CEMA−HEMA) part of the cylindrical aggregates either. Averaging over ∼100 aggregates, we obtained the average TEM diameters of 26.0 ± 2.4 and 26.1 ± 2.5 nm for the cylindrical aggregates before and after the heat treatment. Despite the ineffectiveness of the heat treatment in improving the TEM P*t*BA/P(CEMA−HEMA) core/shell contrast, it was essential for the preparation of polymer/Pd/Ni fibers. Without it, the polymer/Pd fibers were found to aggregate and precipitate from the Ni plating solution. Since divalent cations such as Ni^{2+} and Ca^{2+} were known to induce the aggregation of nanospheres in water bearing PAA groups via complexation with AA groups of different chains,[23] the improved stability of the heat-annealed fibers in the Ni plating solution suggests an increased degree of P*t*BA segregation into the interior of the triblock cylindrical aggregates.

A freshly precipitated PGMA−P(CEMA−HEMA)−P*t*BA sample before vacuum drying was always used and stirred in water to prepare the cylindrical aggregates mainly to improve the yield of sample dispersion in water. After vacuum-drying, the PGMA−P(CEMA−HEMA)−P*t*BA sample transformed into dense lumps that were difficult to disperse in water. With use of our sample preparation protocol, the yield of polymer dispersion was ∼80%. While we might be able to improve the yield of polymer dispersion even further by extending the stirring time, diluting the sample, or increasing the dispersion temperature, we did not investigate these possibilities further for the sufficiently high yield of the cylindrical aggregates.

Aside from this direct water dispersion method, we also tried another sample preparation protocol. It involved dissolving the triblock in pyridine first and then adding water. Above the water content of 95%, the sample was dialyzed against water to remove pyridine. Unfortunately, the indirect protocol yielded only spherical aggregates. The fact that the morphology of the final aggregates depended on the preparation method utilized made the origin (kinetic vs thermodynamic origin) of our cylindrical aggregates unknown. This explains why we have so far referred to the particles as aggregates and not micelles.

PGMA−P(CEMA−HEMA)−PAA Nanotubes. Nanotube preparation involved first the photo-cross-linking of the P(CEMA−HEMA) layer and then the selective hydrolysis of P*t*BA, which involved reactions that have been performed extensively in our group. While the photo-cross-linking reaction was trivial involving irradiation of the sample by UV light, the optimization of the CEMA conversion invoked several trials. Too low a CEMA conversion did not allow the locking of the cylindrical structure and too high a CEMA conversion slowed the transport of Pd(II) and Ni^{2+} across the P(CEMA−HEMA) layer. We found that a CEMA conversion of ∼30% was optimal for the targeted preparation.

The rate of Ni plating also varied with the degree of HEMA cinnamation *x*. When the PHEMA block was fully cinnamated, Ni plating into the nanotube core was difficult probably for the slow transport of the plating components across the PCEMA layer.

The seemingly simple hydrolysis of P*t*BA created initially much headache for us. P*t*BA is readily and quantitatively hydrolyzed by trifluoroacetic acid in CH_2Cl_2.[24] Unfortunately, this treatment produced nanotubes that were not dispersible in water. This difficulty was overcome only with the addition of the cation scavenger triethylsilane during the hydrolysis. Our speculation is that the *tert*-butyl cations produced in the absence of triethylsilane initiated side reactions with PGMA and HEMA. Unfortunately, the exact reaction pathways and products were difficult to identify by traditional techniques such as NMR for their low sensitivity.

Palladium Loading. Pd(II) was loaded into the nanotube core by stirring the nanotubes with $PdCl_2$ in DMF. Pd(II) entered the tube cores most likely for its complexation with the AA groups. The nanotubes were readily separated from the free Pd(II) by filtration through a 0.2-μm filter. We monitored the kinetics of Pd(II) sorption via analysis of the residual Pd(II) amount in the filtrate. Figure 2 shows the kinetic data with the amount in either milligrams of Pd(II) sorbed by each gram of nanotubes or moles of Pd(II) by

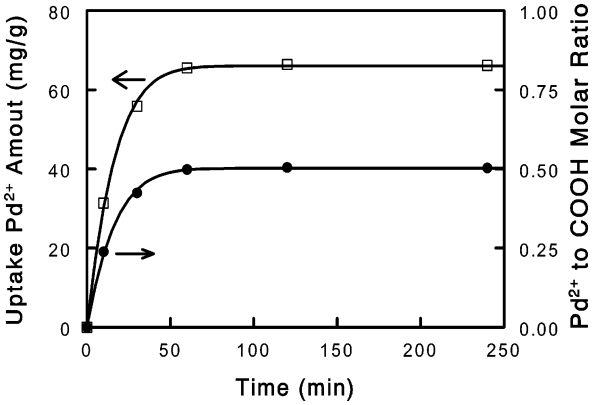

Figure 2. Kinetics of Pd(II) uptake by the PGMA−P(CEMA−HEMA)−PAA nanotubes.

Table 3. TGA Data and Results for the PGMA−P(CEMA−HEMA)−PAA Nanotubes and the Hybrid Nanofibers

sample	polymer/Pd to Ni^{2+} wt ratio	residual wt %	Pd wt %		Ni wt %	
			exptl	theor	exptl	theor
tubes		6.2%				
polymer/Pd fibers		12.3%	6.6%	6.2%		
polymer/Pd/Ni fiber 1	1.00/0.100	20.4%			9.1%	9.1%
polymer/Pd/Ni fiber 2	1.00/0.400	37.2%			28.5%	28.6%
polymer/Pd/Ni fiber 3	1.00/1.00	57.8%			52%	50%
polymer/Pd/Ni fiber 4	1.00/2.00	72.7%			68%	67%
polymer/Pd/Ni fiber 5	1.00/4.00	85.0%			83%	80%

each mole of COOH groups. The sorption equilibrium was established within ∼50 min. Since Pd(II) was used in excess in this case, 1 mol of Pd(II) was complexed in this case with approximately two moles of COOH groups at the sorption equilibrium, in agreement with the stoichiometry [Pd(II)]/[COOH] = 1/2 or the Pd(II) sorption result for microspheres bearing internal PAA chains.[25] Based on data of Figure 2, we always equilibrated Pd(II) with the nanotubes overnight to prepare polymer/Pd/Ni nanofibers. To minimize Pd(II) use and to maximize Ni deposition, we used in these cases Pd(II) amounts, in the Pd(II) loading solution, less than the stoichiometric ratio [Pd(II)]/[COOH] = 1/2.

Pd(II) inside the nanotube cores was reduced by $NaBH_4$. After Pd(II) reduction and sample cleaning, we performed a TGA analysis of a sample from the kinetic run with a sorption equilibrium time of 240 min. This yielded a Pd amount of 6.6 wt % (Table 3), which is in reasonable agreement with 6.2% reported in Figure 2 considering that the polymer/Pd fibers may not be perfectly free of impurities such as Cl^-. Shown in Figure 3a is a TEM image of a polymer/Pd nanofiber sample with 2.1 wt % of Pd. Most of the palladium nanoparticles were produced inside the nanotube cores as expected. A closer examination of the image reveals that some of the particles take an elongated shape, reflecting the templating effect of the nanotube cores.

There have been several reports on the reduction of Pd(II) in the PVP core of PS−PVP micelles, where PS−PVP denotes polystyrene-*block*-poly(4-vinyl pyridine).[26] The general consensus was that the use of hydrazine as the reductant produced larger Pd particles. We have used also hydrazine at concentrations ranging from 0.5% to 40 vol % in water as the reductant. The surprising discovery was that the use of hydrazine even at 40 vol % led to the formation of many Pd nanoparticles outside the nanotubes. Our speculation is that hydrazine was a strong base and slow reductant. Its addition helped weaken the bonds between Pd(II) and the carboxyl groups and the release of Pd(II) from the nanotube cores.

Polymer/Pd/Ni Nanofibers. The loaded palladium catalyzed the electroless deposition of Ni inside the nanotubes to yield polymer/Pd/Ni nanofibers. Table 3 gives the Ni contents calculated from TGA analysis of the polymer/Pd/Ni fibers prepared using different feed weight ratios of the polymer/Pd nanofiber and Ni^{2+} in the initial Ni plating solutions. As the Ni^{2+} to polymer/Pd nanofiber feed weight ratio increased, the final plated Ni amount increased. The fact that the determined Ni amounts agreed well with those predicted from the feed ratios suggests that we could tune the Ni amount plated by adjusting the composition of the initial plating mixture.

While we could prepare, in principle, fibers with any weight fraction of Ni, only fibers that had less than ∼31 wt % of Ni dispersed well in water as judged by the naked eye. The decreased dispersion was most likely caused by the increased degree of fiber bundling at high Ni contents. Our TEM observations indicated that the fibers existed mostly as individual fibers or were mostly separated from one another like those shown in Figure 3b at 31 wt % of Ni. At 52 wt % of Ni, we could still detect single fibers at the edges of fiber bundles or aggregates (Figure 3c). At 68 wt % of Ni, it became almost impossible to find single fibers and the observation of small fiber bundles such as those seen in Figure 4d became a rare event as well.

While the greater tendency for fiber bundling could result partially from the increased van der Waals attraction between fibers with increasing Ni content,[27] the dominant interaction here should be the magnetic dipole−dipole attraction, which increases for spherical particles to the sixth power of the radius of particles.[28] A comparison between Figures 3a and 3b reveals that the metal particles in Figure 3b are on the average bigger, suggesting thus the growth of Ni on the original Pd particles. As Ni content increased, we noticed from Figure 3b to 3c a further increase in the average size and length of the metal particles. Many large metal particles, e.g., >50 nm, are seen in Figure 3d. These large particles seem to form from the overgrowing of the tube template by Ni. While the TEM images suggest a size increase for the metal particles with Ni content, the images should, however, not be over-interpreted first for the small sampling size of the TEM technique and second for the fact that the TEM images shown in Figure 3c and 3d are not representative of these samples, which formed mostly aggregates.

For dispersibility issues, only fibers with ≤31% Ni were characterized in any further detail. The appearance of such a polymer/Pd/Ni dispersion is captured in a photograph (Figure 4a). It is black and is very stable in water. After shaking and then leaving the sample standing for 24 h, we noticed no visible precipitation or aggregation in the sample. Upon placement of it next to a magnet, the particles got slowly captured. Figure 4b shows the status of the dispersion after it has been placed next to a 0.47-T magnet for 4.5 h.

(28) Butter, K.; Bomans, P. H. H.; Frederik, P. M.; Vroege, G. J.; Philipse, A. P. *Nat. Mater.* **2003**, *2*, 88.

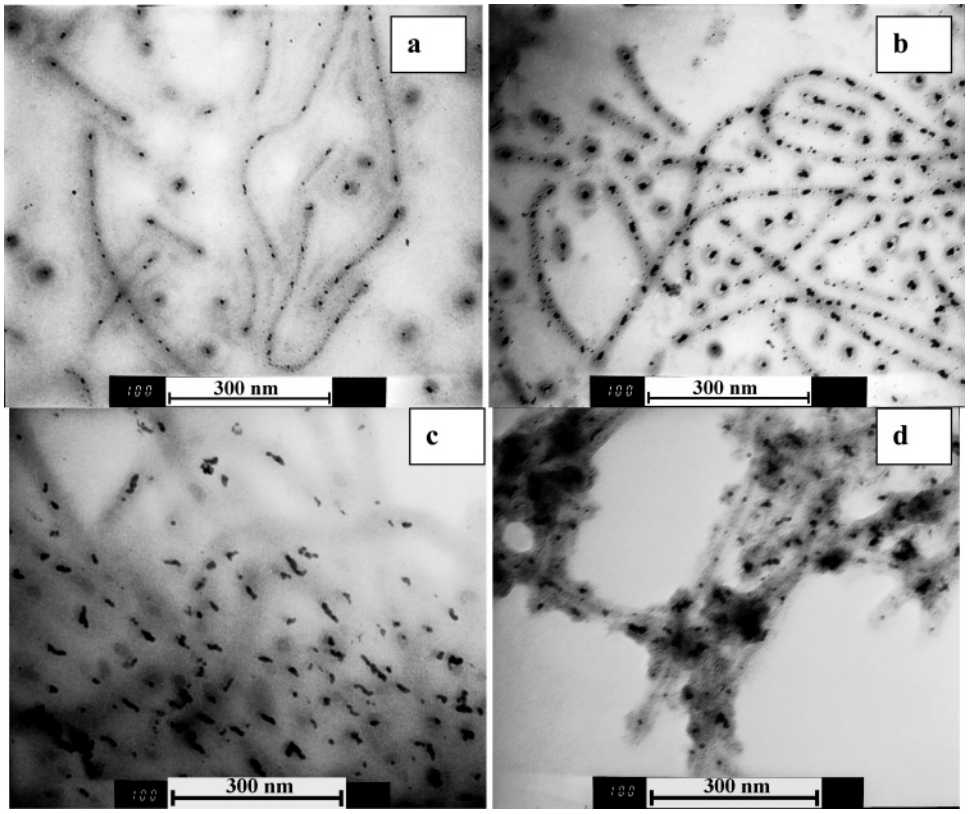

Figure 3. TEM images of polymer/Pd and polymer/Pd/Ni nanofibers. The Pd and Ni weight fractions in the hybrid nanofibers were at 2.1 wt % Pd (a), 31 wt % Ni (b), 52 wt % Ni (c), and 68 wt % Ni (d), respectively.

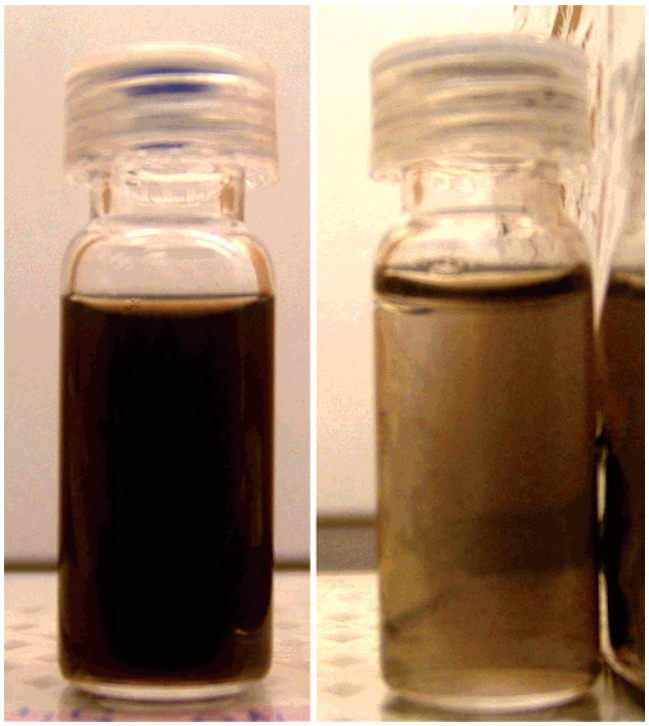

Figure 4. Photographs showing an aqueous polymer/Pd/Ni nanofiber dispersion before and after being placed next to a 0.47-T magnet for 4.5 h.

We have also obtained room-temperature magnetization curves for the solid polymer/Pd/Ni nanofibers at different Ni contents. Figure 5 shows a magnetization curve for a sample with 31 wt % Ni. The saturation magnetization of this sample is 12.5 emu/g of Ni. The remanent magnetization and coercivity are 2.0 emu/g and 0.026 kOe, respectively.

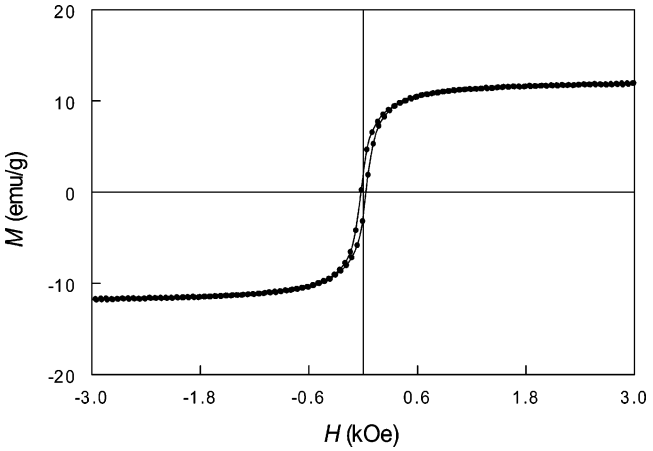

Figure 5. Magnetization curve of a solid polymer/Pd/Ni nanofiber sample at 298 K.

Thus, the fibers contained Ni particles that were ferromagnetic with sizes above the superparamagnetic limit, which is 15 nm for spherical Ni particles.[29] Fortunately, the presence of a small number of such larger particles did not lead to visually noticeable aggregation of the fibers.

The saturation magnetization of bulk Ni is 54.39 emu/g,[30] which is more than 4 times the value of our sample. A saturation magnetization lower than that for bulk materials is normal for nanoparticles. Typical reasons for this include the reaction or complexation of the surface atoms of magnetic nanoparticles with surfactant which may create a magneti-

(29) Du, Y. W.; Xu, M. X.; Shi, Y. B.; Lu, H. X. *J. Appl. Phys.* **1991**, *70*, 5903.
(30) Gray, D. E. *American Institute of Physics Handbook*; McGraw-Hill: New York, 1972.

cally dead layer.[31] With a significant fraction of surface atoms any crystalline disorder within the surface layer may also lead to a significant decrease in nanoparticle saturation magnetization.

IV. Conclusions

Stirring a PGMA−P(CEMA−HEMA)−P*t*BA sample in water produced mostly cylindrical aggregates consisting of PGMA corona, P(CEMA−HEMA) intermediate layer, and P*t*BA core. The aggregate structure was locked in by photo-cross-linking the P(CEMA−HEMA) intermediate layer. Poly(acrylic acid)-lined tubes were obtained after hydrolyzing the *tert*-butyl groups from P*t*BA. Such nanotubes served as nano test tubes to enable the loading of Pd(II) via binding with PAA. Pd(0) nanoparticles were produced after Pd(II) reduction. Pd(0) served as the catalyst for further Ni deposition by electroless plating. The polymer/Pd/Ni hybrid nanofibers at a Ni content less than ∼31 wt % dispersed well in water and were captured slowly by a magnet. Such fibers may find applications in medical diagnostics[32] and other areas.

Acknowledgment. NSERC of Canada is gratefully thanked for sponsoring this research. Dr. Zhao Li is thanked for synthesizing the triblock used.

CM051548D

(31) Burker, N. A. D.; Stover, H. D. H.; Dawson, F. P. *Chem. Mater*. **2002**, *14*, 4752

(32) See, for example, Liu, G. J.; Yan, H. S.; Zhou, J. Y.; Law, S. J.; Jiang, Q. P.; Yang, G. H. *Biomacromolecules* **2005**, *6*, 1280.